The temporal dynamics of response inhibition and their modulation by cognitive control

Liisa Raud[1], René J. Huster[1, 2]

[1]Department of Psychology, University of Oslo, Oslo, Norway

[2]Psychology Clinical Neurosciences Center, University of New Mexico, Albuquerque, USA

Running title: Selective inhibition and cognitive control

Keywords: EMG, N1, N2, P3, SOBI, stop signal task

Correspondence:

René J. Huster
Department of Psychology,
University of Oslo
Norway
Tel: +47-228-45162
E-mail: rene.huster@psykologi.uio.no

Published in Brain Topography, 2017

doi: 10.1007/s10548-017-0566-y

Abstract

Behavioral adjustments require interactions between distinct modes of cognitive control and response inhibition. Hypothetically, fast and global inhibition is exerted in the reactive control mode, whereas proactive control enables the preparation of inhibitory pathways in advance while relying on the slower selective inhibitory system. We compared the temporal progression of inhibition in the reactive and proactive control modes using simultaneous electroencephalography (EEG) and electromyography (EMG) recordings. A selective stop signal task was used where go stimuli required bimanual responses, but only one hand's response had to be suppressed in stop trials. Reactive and proactive conditions were incorporated by non-informative and informative cues, respectively. In 47% of successful stop trials, subthreshold EMG activity was detected that was interrupted as early as 150 ms after stop stimulus presentation, indicating that inhibition occurs much earlier than previously thought. Inhibition latencies were similar across the reactive and proactive control modes. The EMG of the responding hand in successful selective stop trials indicated a global suppression of ongoing motor actions in the reactive condition, and less inhibitory interference on the ongoing actions in the proactive condition. Group-level second order blind separation (SOBI) was applied to the EEG to dissociate temporally overlapping event-related potentials. The components capturing the N1 and N2 were larger in the reactive than the proactive condition. P3 activity was distributed across four components, three of which were augmented in the proactive condition. Thus, although EEG indices were modulated by the control mode, the inhibition latency remained unaffected.

Introduction

Response inhibition serves to regulate behavior by suppressing inappropriate actions that no longer correspond to the demands of the environment. Adequate behavioral flexibility additionally demands intricate interactions between inhibition and distinct modes of cognitive control. Whereas proactive control refers to the sustained shaping of attentional processing through goal-relevant information, reactive control reflects transient adaptations in response to salient or imperative events (Braver 2012). According to a prominent theory, reactive and proactive control have distinct effects on the inhibitory system, with reactive control activating the fast hyperdirect motor pathway that results in a rapid inhibitory pulse over all ongoing processes, whereas proactive control operates via the indirect motor pathway, resulting in slow but specific inhibition of the target action (Aron 2011).

The global-selective inhibition distinction is often studied by a modified stop signal task where the go stimuli require a bimanual speeded response and the occasional stop stimulus signals for the suppression of either both hands (global stop), or only one hand while the other response is still to be executed (Coxon et al. 2007; Aron and Verbruggen 2008). However, this behavioral manipulation appears to be insufficient to dissociate between the global and selective inhibitory systems at the neural level. Rather, the so-called restart model states that global inhibitory system suppresses all ongoing actions also in the selective stop trials, and is then followed by the newly generated correct response (Coxon et al. 2007; Macdonald et al. 2012, 2014). This is evidenced behaviorally by remarkable costs on reaction times of the still responding hand, known as the stopping interference (SI) effect (Aron and Verbruggen 2008; Ko and Miller 2011, 2013). Similarly, transcranial magnetic stimulation (TMS) studies have showed temporarily reduced corticomotor excitability of the responding hand in response to the selective stop signal (Macdonald et al. 2014). Proactive control, however, appears to modulate inhibition specificity. Providing preparatory cues significantly reduces the SI effect (Aron and Verbruggen 2008; Claffey et al. 2010; Smittenaar et al. 2013; Lavallee et al. 2014) and results in a more selective suppression of corticomotor excitability as measured by the TMS (Claffey et al. 2010; Cai et al. 2011; Majid et al. 2012). Counter-intuitively, preparatory cueing can also lead to slower inhibition as measured by the stop signal reaction times (SSRT), putatively due to its implementation via the anatomically more complex indirect pathway, as opposed to the fast but unspecific hyperdirect pathway (Aron and Verbruggen 2008; Claffey et al. 2010; Lavallee et al. 2014). This introduces the dichotomy between global and selective neural inhibitory systems that may not correspond to the behavioral distinction (stop one hand vs. stop both hands), but is

implicitly equivalent to inhibition in the reactive and proactive control modes, respectively (Aron 2011; Majid et al. 2013). The generalizability of this dichotomy needs further study, however, not least since faster SSRTs for the proactive than for reactive mode have been observed as well (Smittenaar et al. 2013, 2015), and subcortical neural activation patterns involving both indirect and hyperdirect pathways have been reported for reactive response inhibition (Jahfari et al. 2011) .

The SSRT, typically estimated to be around 200-300 ms, is derived on the basis of the independent horse race model where go and stop processes compete against each other and whichever "wins the race" determines the outcome (Logan and Cowan 1984; Band et al. 2003). Although its validity has been demonstrated in the standard stop signal task (Congdon et al. 2012; Verbruggen et al. 2013), the underlying assumption of independence between stop and go processes appears to be violated in the more complex versions of stop signal tasks (Schall and Godlove 2012; Gulberti et al. 2014; Bissett and Logan 2014; Verbruggen and Logan 2015). In addition, as the SSRT represents the finishing time of the stop process, it acts as a compound measure of multiple cognitive and motor processes (Verbruggen and Logan 2015). Correspondingly, transcranial magnetic stimulation studies showed a decrease in corticomotor excitability as early as 130-180 ms after stop stimulus presentation (Coxon et al. 2006; van den Wildenberg et al. 2010; Macdonald et al. 2014). Relying solely on the SSRT as a measure of individual inhibition latency is therefore problematic and a complementary outcome variable is much desired. In tasks with several competing response tendencies, subthreshold muscle activation can be detected in the electromyography (EMG) recordings of the response effectors even in the absence of an overt response (De Jong et al. 1990; Hasbroucq et al. 1999; Burle et al. 2002). The latency of the interruption of this subthreshold EMG activity in successful stop trials may thus serve as an assumption-free physiological measure of inhibition latency.

EEG is well-suited to investigate neural processes where temporal information is of central interest; yet, identifying an unambiguous index of inhibition has proved challenging (Huster et al. 2013). Most often, modulations in the event-related potentials (ERP) N1, N2 and P3 are reported, with the N1 reflecting sensory processing sensitive to top-down attentional modulation (Bekker et al. 2005a; Boehler et al. 2009; Langford et al. 2016a, b), and the N2 being associated with conflict monitoring and interference processing, as it is highly susceptible to stop stimulus probabilities and stimulus-response compatibility (Nieuwenhuis et al. 2003; Donkers and van Boxtel 2004; Enriquez-Geppert et al. 2010). The P3 onset correlates strongly with the SSRT and was therefore suggested to be an online indicator of response inhibition (Wessel and Aron 2014; Wessel et al. 2016), yet its continuing

development after the SSRT itself would rather support its role in sustained attention and context updating (Filipović et al. 2000; Dimoska et al. 2003; Polich 2007). Kenemans (2015) has suggested a further clarification by attributing the role of the P3 to merely reactive inhibition, triggered in a generic fashion by any novel stimulus. Yet, experimental results have indicated an increased P3 in proactive inhibition (Greenhouse and Wessel 2013; Schevernels et al. 2015). A major limitation of the standard ERP analysis is that ERPs reflect summed neural activity from various neural generators, which limits their potential to dissociate functional processes that occur close in time (Nunez et al. 1997). In effect, blind source separation (BSS) techniques that aim to recover the activity from distinct sources otherwise measured as mixed signals at scalp electrodes, have been immensely successful in identifying activity from a single cortical area, networks of brain regions as well as artefact sources (Hyvärinen and Oja 2000; Onton et al. 2006). Such BSS techniques have suggested that several temporally overlapping components beyond the N2/P3 complex may support inhibition (Huster et al. 2014; Albares et al. 2014; Huster et al. 2016). As of yet, the EEG decomposition of selective stopping has not been investigated.

We conducted simultaneous EEG and EMG measurements on healthy participants performing a selective stop signal task tapping both, reactive and proactive modes of cognitive control. Behaviorally, we expected longer SSRTs and smaller SI effects in the proactive control condition as a support for the slowly operating selective inhibitory system. These effects were expected to be paralleled by the EMG, with a later EMG interruption latency in the stopped hand and less interference on the response hand EMG activity in the proactive condition. Regarding the EEG, we expected that the ERPs typically seen in the standard stop signal task would also be evident in selective inhibition. However, we expected their amplitudes to be modulated by cognitive control modes with a stronger N2 in the reactive mode as an indicator of increased conflict between go and stop representations, and stronger N1 and P3 in the proactive mode reflecting increased load for sustained attentional modulation. A thorough correlational analysis was performed to establish the associations of the ERP components with reactive and/or proactive inhibition. Prior to the analysis, EEG data was subjected to group-level second-order blind identification (group-SOBI), allowing a precise distinction of temporally overlapping ERP components.

Methods

Participants

33 volunteers (aged 20-29 with the mean age of 25; 14 females and 19 males) participated in the experiment. All participants were right-handed as confirmed by a handedness inventory (Oldfield 1971), had normal or corrected-to-normal vision and reported no history of neurological or psychiatric disorders. Data from three participants were discarded due to technical issues during data acquisition. Informed consent was obtained from all participants and they were paid a compensation for their contribution. The study was approved by the institutional review board of the University of Oldenburg.

Task and procedure

The participants performed a selective stop signal task incorporating reactive and proactive conditions (Figure 1). Task presentation was controlled using the Presentation software (version 14.8, Neurobehavioral Systems). Participants were seated in an armchair in an electrically shielded and sound attenuated chamber and the stimuli were presented at the screen at approximately one meter distance from the participants' eyes. Responses were given via a response pad. A central fixation-cross was presented throughout the experiment. The go-stimuli were two simultaneously presented white circles with a diameter of 2.5 cm and a distance of 10 cm between them, to which the participants had to respond with bimanual button presses. In stop trials (40%), a red circle occurred either at the left or at the right position previously occupied by one of the go stimuli. Then, participants had to suppress the response of the hand corresponding to the side of the stop stimulus, but to continue the response of the other hand. That is, if the stop signal occurred in the left, participants had to stop their left hand response but execute the right hand response and vice versa.

All stop trials required the selective stopping of one, but not the other hand. Thus, the specificity of the underlying inhibitory mechanisms was expected to be modulated by the reactive and proactive control modes, incorporated by non-informative and informative cues, respectively. In half of the trials, the cue was non-informative ("xxx"; reactive condition), whereas in the other half of the trials an arrow was pointing either to the left or to the right, indicating where a stop signal might occur. Thus, with these spatially informative cues participants could prepare for the potential stop stimulus

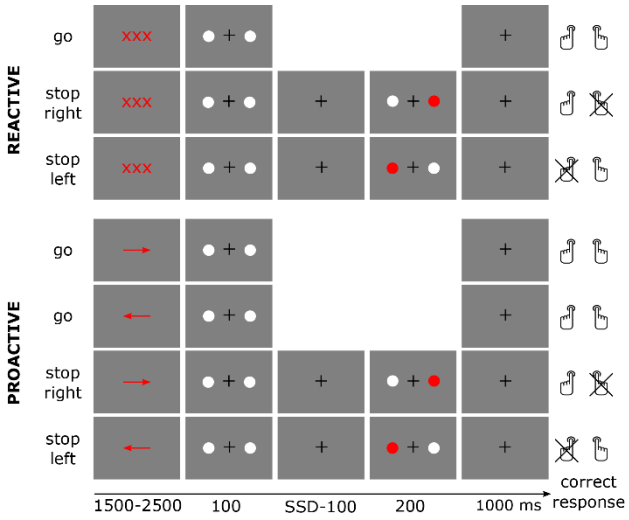

Fig. 1. Selective stop signal task in the reactive and proactive condition, implemented by non-informative and informative cues, respectively; all trials were counterbalanced and presented in pseudorandomized order

in advance (proactive condition). All cues were congruent, so proactive stop left hand trials were always preceded by an arrowhead pointing to the left and vice versa for proactive stop right trials.

A trial started with the presentation of a cue with randomized duration between 1500 and 2500 ms. After the cue offset, go stimuli were presented for 100 ms. On stop trials, stop stimuli were shown after the experimentally adapted stop-signal delay (SSD) for 200 ms. To achieve a stop trial accuracy of 50%, the SSD was adjusted separately for reactive and proactive conditions (collapsed over stop left and right trials) according to the staircase method of the horse-race model (Band et al. 2003). The initial SSD was set to 250 ms and it was increased by 50 ms if the response in the previous stop trial was correct, and decreased by 50 ms if the previous stop trial response was false. A response window with a duration of 1000 ms terminated all trials.

Altogether, 700 trials were presented, half of which were reactive while the other half were proactive trials. Stop trials were further divided equally into stop left hand and stop right hand trials within both conditions. This resulted in 140 stop trials per condition with 70 stop left and 70 stop right trials.

The instructions were given in written form before the onset of the experiment. It was stressed additionally that it was not possible to always react correctly. Firstly, all participants completed a training session of 5 minutes followed by the experimental session, altogether lasting for approximately 55 minutes. A pause of self-regulated duration was introduced after every 3.5 minutes during which feedback was presented. Participants were asked to respond faster if the average reaction time was longer than 600 ms. Instantaneous feedback was presented in case no response was given in a go trial, or when the reaction time of a go trial exceeded 1000 ms, prompting the participants to respond faster. In addition, the central fixation cross turned red directly after the trial when left and right hand responses were not simultaneous, that is their difference was longer than 70 ms.

Data acquisition

Simultaneous EEG and EMG recordings were taken using a BrainAmp system (Brainproducts, München, Germany). Data was low-pass filtered online at 250 Hz for EEG and at 1000 Hz for EMG channels and recorded continuously at a sampling rate of 2500 Hz. All neurophysiological data was further processed offline using in-house MATLAB scripts and the EEGLAB toolbox (Delorme and Makeig 2004).

EEG activity was measured at 31 electrodes placed according to the international 10-20 system. An additional electrode was placed under the right eye to control for ocular artefacts. All EEG electrodes were referenced against the nose-tip electrode and their impedances were kept below 5 kOhm.

Bipolar surface EMG recordings were performed on the thumb muscles of both hands. Two Ag/Cl-electrodes were placed on the *abductor pollicis brevis* with the ground electrode placed on the left arm. The set-up included an additional electrode pair on the dorsal side of the hand to record the activity of the same muscles, but due to the weaker signal and larger noise from the neighboring muscle groups, these recordings were not analyzed any further. Appropriate support for the participants' arms was provided to reduce spurious muscle tension during rest.

Data analysis

Behavioral analysis

All trials were sorted according to the given response into correct go trials, correct stop trials, and false alarms (unsuccessful inhibition). Go trials without responses, asynchronous responses (reaction time difference between left and right hand response > 70 ms) or only one-hand responses were discarded from the analysis. Similarly, stop trials without any response or with a response of the wrong hand (e.g. only left hand response on stop-left trials) were omitted. The following behavioral measures were extracted: go trial reaction times (go-RTs), false alarm reaction times (fa-RTs), unstopped hand reaction times (responding hand on stop trials; stop-RTs), and SI (the difference between stop-RTs and go-RTs). As an initial analysis revealed no differences between left and right hand responses, all analyses were collapsed over stop left and stop right trials. SSRTs were estimated for both the reactive and the proactive condition using the so-called mean method, i.e. subtracting the mean SSD from the go-RTs averaged over both hands. The mean method is among the most common methods for estimating the SSRT, and it is relatively robust when the horse race

model assumptions have been met (Congdon et al. 2012). However, even subtle differences in go-reaction time distributions can lead to spurious effects, especially in case of strategic slowing (Boehler et al. 2012; Verbruggen et al. 2013). Thus, we also estimated the SSRTs using the block-wise integration method (50 trials per block). As the results were almost identical to the mean method (correlations between the mean and integration methods were 0.94 for the reactive and for the 0.96 proactive condition, respectively), only the results of the mean method are reported. All behavioral measures in the reactive and proactive condition were compared using paired samples t-test.

Electromyography

Preprocessing. EMG channels were low-pass filtered at 250 Hz and high-pass filtered at 1 Hz. Data was resampled to 500 Hz and segmented with a time-window of -200 to 1000 ms relative to go stimuli in go trials and stop stimuli in stop trials. The epochs were baseline corrected to the pre-stimulus time-window. A temporal smoothing procedure was applied to the EMG activity: for each time point, the root mean square (RMS) was calculated and a moving average over +/-5 neighboring data points was computed. The single trial post-stimulus time-courses were then divided point-wise by the trial specific average of the pre-stimulus period of -200 to 0 ms. The resulting single trial time-courses thus represent the ratio of the RMS-transformed signal to the pre-stimulus baseline. These were averaged across all trials. To validate the EMG parametrization procedure, a correlation analysis was performed between the peak latencies of the single subject response-related EMG time-courses and the reaction times.

Statistical assessment. An automatic algorithm for the detection of the subthreshold EMG bursts in single trials was applied to the stopped hand EMG to estimate their occurrence frequency (modified from Cohen and van Gaal 2014). A burst was identified when the derivative of the RMS-transformed time-course between the onset of the stimulus and stop-RT of the particular trial exceeded two; that is, there occurred a sudden change in the signal with a data point being twice as large as the preceding one. The resulting frequencies were quantified as percentages of all successful stop trials per participant and were further compared between reactive and proactive conditions with a paired samples t-test.

Peak latencies of the subthreshold (stopped hand) EMG between stop stimulus onset and the average stop-RTs were extracted from the subject-specific time-courses and compared by paired samples t-test. Additionally, subthreshold EMG latencies were correlated with the SSRT. As we expected a positive correlation, the one-tailed test result will be reported.

To further investigate the dynamics of EMG activity, the full time-courses were subjected to an exploratory analysis using point-wise permutation tests with Monte Carlo label switching (10 000 iterations, two-tailed). We compared the reactive-proactive differences within both, stopped and unstopped hand EMG activity. The resulting p_N-values were corrected for multiple comparisons using the false discovery rate (fdr) procedure with an alpha level of 0.05 (Benjamini and Hochberg 1995). Further, a cluster of significant values had to span over a time-window longer than 30 ms to be considered significant.

To elucidate the findings from the permutation testing, a further analysis was carried out on the peak amplitudes of the response-related EMG in go and stop trials on a post-hoc basis. The mean amplitudes of +/-5 data points around the peak EMG responses were extracted from go trials and from successful stop trials, aligned to the go stimuli. Paired samples t-tests were used to contrast the EMG amplitudes in go and stop trials, and in the reactive and proactive condition in stop trials.

Electroencephalogram

Preprocessing. EEG data was low-pass filtered at 75 Hz and high-pass filtered at 0.1 Hz, and resampled to 500 Hz. For each subject, an independent component analysis (ICA) was computed using EEGLAB's built in infomax algorithm (Delorme and Makeig 2004). Components representing eye movements and muscle artefacts were removed and the remaining components were back-projected to the EEG channel domain. Trials with non-systematic residual artefacts were removed manually (4 trials (0.63%) per subject on average, ranging from 0 to 21 trials across all subjects). The data was segmented and time-locked to go stimuli in go trials and stop stimuli in stop trials with a time window of -200 to 1000 milliseconds, and then baseline corrected to the mean of the pre-stimulus period. This allows the investigation of stimulus-evoked effects independently from the cue-evoked activity by equalizing the signal offsets prior to the stimulus presentation. However, as some differences between reactive and proactive conditions are expected also in the baseline activity, we note that this choice of baseline may disregard any non-additive interaction effects regarding the pre- and post-stimulus activity.

SOBI. SOBI is a blind source separation (BSS) technique, based on the joint diagonalization of a set of covariance matrices (Belouchrani et al. 1997), for the estimation of source signals that are linearly mixed in the observed variables. In case of EEG data, BSS techniques relying on higher order statistics, i.e. ICA, are most commonly applied on single subject data for artifact rejection. More recently, procedures have been developed that achieve the decomposition of aggregate data from multiple

subjects (Eichele et al. 2011). Thus, group-level BSS techniques, often used in combination with data reduction steps, result in a single set of components that capture the representative activity from neural sources commonly expressed across the whole sample. Each participant's individual manifestation of a particular component can then be reconstructed via the resulting de-mixing matrix, allowing for statistical interference across subjects or conditions. Here, SOBI was preferred over ICA since it is more robust when the events of interest include temporal jitter, as in case of motor responses with variable reaction times (Huster et al. 2015). Additionally, SOBI has been shown to be more robust to variations in the underlying mixing matrix, likely to exist in the aggregate multi-subject data due to inter-individual variability in brain and skull structures (Lio and Boulinguez 2013).

To compute a group-level SOBI, an equal number of trials across participants is necessary. Thus, each participant's data was randomly subsampled, selecting 29 trials (minimal number of artifact-free trials across all conditions and participants) per each condition and trial type (reactive go; proactive left go; proactive right go; reactive left stop; reactive right stop; proactive left stop; proactive right stop). Additionally, 20 unsuccessful stop trials per each stop condition were included for each participant. The final aggregate dataset thus consisted of 283 trials per participant. To compensate for inter-trial variability in response-related source onsets, the trial order for each condition was sorted across subjects according to the reaction times in go trials, unstopped hand reaction times in successful stop trials, and false alarm reaction times in unsuccessful stop trials.

Group-SOBI was applied to the EEG, preceded by two consecutive principal component analysis steps (PCA; single subject and group level) as a means of data reduction (Eichele et al. 2011; Huster et al. 2015). Firstly, for each participant, all trials were vertically concatenated and z-standardized over channels, resulting in a two-dimensional matrix with electrodes as rows and time-points as columns spanning all 283 trials. This was then entered into a subject-specific PCA. 15 PCs were selected from each participant, on average accounting for 99% of the variance in the single-subject data. These 15 components were extracted from each subject's data, concatenated vertically (along the dimension originally representing channels), and entered into a second, group-level PCA. Again, 15 group-PCs were extracted and subjected to SOBI (with temporal lags up to 50 data points or 100 ms), resulting in 15 group-level component time-courses. Finally, single-subject activation of those components were reconstructed by matrix multiplication of the original single-subject EEG time-courses with the weight matrices resulting from the two preceding PCA's and SOBI (see Eichele et al. 2011; Huster et

al. 2015 for details). The single-trial component time-courses were baseline corrected and low-pass filtered with 35 Hz to increase the signal-to-noise ratio.

Component selection. From all of the resulting components, we selected those components best capturing ERPs known from previous research to be modulated in response inhibition tasks. That is, we identified the components best capturing the N1, N2 and P3 based on their typical topographies and time-courses. To verify the component selection, the component time-courses were first correlated point-wise with the original ERPs within the relevant time-window as defined by the grand averages (100-300 ms for the N1 and N2; 100-500 ms for the P3), and then squared and averaged over all time-points. This resulted in an estimate of the variance explained of the original ERP by the particular component. In case of the P3, there were four components that fulfilled the criterion of marked positivity at around 300 ms over fronto-central or centro-parietal electrodes; these were all included for further statistical assessment. Since the signs of SOBI time-courses and loadings are somewhat arbitrary, the time-courses and topographies of three components (components 6, 11 and 12) were sign-inverted for visualization purposes and to ease the interpretation, so that they would agree with the standard presentation of the N2 and P3.

Statistical assessment. Mean amplitudes for each component in the time-windows around the local peaks of the grand averages were extracted to test for experimental effects on component activity. The time-windows were specified as 150-250 ms for the N1 (component 4) and 200-300 ms for the N2 (component 6). In case of the P3, four different components were selected with following time-windows for statistical assessment: 300-400 ms (component 11), 250-400 (component 12), 350-450 ms (component 10), 250-350 ms (component 8). The mean amplitudes were entered into a repeated-measures ANOVA with factors *trial* (go, stop) and *condition* (reactive, proactive); significant effects were followed up by Bonferroni-Holm post-hoc tests.

The associations of the EEG components with inhibitory processes were investigated by correlating their mean amplitudes with the SSRTs and subthreshold EMG latencies. Because recent evidence highlights the importance of component onset times, as opposed to mere peak amplitudes, the correlational analysis was additionally performed on the components' onset latencies. The onsets were defined as the time-point when 10% of the positive area under the curve (shifted upwards by the minimum value in the time-window to also include the activity below the baseline) was reached within the same broader time-windows as defined previously for the assessment of the variance explained (100-300 ms for the N1 and N2; 100-500 ms for the P3).

Results

Behavioral data

The behavioral and EMG results are summarized in Table 1. Overall, the participants performed well in the task as shown by the correct go trial response rates of 95.9% and 91.9% in the reactive and proactive condition, respectively. The accuracies in the proactive were significantly smaller than in the reactive condition ($t(29) = 5.43$, $p < 0.01$, $d = 0.99$). Post-hoc analysis of the types of errors demonstrated that participants made more asynchronous responses (3.1% vs. 2.1%, $t(29) = -3.49$, $p < 0.01$, $d = -0.64$) and responded more often with only one hand (4.2% vs. 1.3%, $t(29) = -4.62$, $p < 0.01$, $d = -0.84$) in the proactive condition, altogether suggesting that participants indeed used the cues to prepare for the looming need for inhibition.

	Reactive	**Proactive**
Behavior		
Go accuracy* (%)	95.9 (0.7)	91.9 (1.0)
Stop response rate (%)	51.9 (0.2)	52.1 (0.3)
Go RT (ms)	642 (19)	646 (20)
False alarm RT (ms)	564 (17)	572 (18)
Stop RT* (ms)	774 (24)	757 (24)
Stopping interference* (ms)	131 (10)	111 (11)
Stop signal delay (ms)	440 (22)	451 (22)
Stop signal reaction time (ms)	203 (5)	195 (6)
Subthreshold EMG		
Detection frequency (%)	46.6 (3.2)	46.8 (2.6)
Peak latency (%)	147 (4)	152 (4)

Table 1. Behavioral and EMG results across reactive and proactive conditions (n = 30). The standard errors are represented in the brackets. RT- reaction time; SI – stopping interference. *significant difference with $p < 0.05$ between the reactive and proactive condition

The go-RTs and fa-RTs were similar across the reactive and proactive condition. The unstopped hand reaction times were longer in the reactive than in proactive condition ($t(29) = 3.03$, $p < 0.01$, $d = 0.55$), resulting in a reduced SI effect in the proactive condition ($t(29) = 3.67$, $p < 0.01$, $d = 0.67$). The fa-RTs were faster than go-RTs both in the reactive ($t(29) = 12.68$, $p < 0.01$, $d = 2.31$) and proactive ($t(29) = 12.75$, $p < 0.01$, $d = 2.33$) condition, and were therefore in a good accordance with the horse race model assumptions. The stop trial accuracies were 52% in both conditions. The SSRTs correlated negatively with the go reaction times in the reactive condition ($r = -0.38$, $p = 0.03$), but not in the proactive condition ($r = -0.17$, $p = 0.38$). The negative correlation in the reactive condition may indicate that the SSRT calculation yielded unreliable estimates. However, similar trends occurred also regarding the go reaction times and the sub-threshold EMG latencies (reactive: $r = -0.31$, $p = 0.09$; proactive: $r = -0.04$, $p = 0.81$), indicating a more complex relationship between go reaction times and inhibition latencies. Although inhibition in the proactive condition was expected to be slower than in the reactive condition, no differences occurred regarding the SSD ($t(29) = -1.52$, $p = 0.14$, $d = -0.28$) nor the SSRT ($t(29) = 1.32$, $p = 0.20$, $d = 0.24$).

Electromyography

EMG results are summarized in Table 1 and the time-courses are shown in Figure 2A and C. The peak latencies of go trial EMG, averaged over both conditions, correlated strongly with the go trial reaction times ($r = 0.94$, $p < 0.01$, one-tailed) and the same was true for the unstopped hand ($r = 0.95$, $p < 0.01$, one-tailed; Figure 2B). Subthreshold EMG activity was detected in 47% of all successful stop trials, and it was interrupted at around 150 ms after stop stimulus presentation with no significant differences between the reactive and proactive modes neither regarding the detection frequencies nor the interruption latencies (Table 1), thus being in a good accordance with the behavioral results. Subthreshold EMG latency correlated with the SSRT both in the reactive ($r = 0.34$, $p = 0.03$, one-tailed) and in the proactive ($r = 0.52$, $p < 0.01$, one-tailed) condition (Figure 2D).

Subthreshold EMG traces of the stopped hand aligned to the stop stimulus were remarkably similar in the reactive and proactive conditions. The unstopped hand EMG, however, revealed interesting temporal dynamics of response execution and inhibition (Figure 2C). Firstly, the interference effect of the stop signal was clearly observable in the activity of the unstopped hand: the rising activation reflecting the executed response was interrupted at around 150 ms and succeeded by another increase in activation. Secondly, there were clear differences between the reactive and proactive

modes: the initial response suppression was reduced in the proactive mode whereas the following rise started earlier and was smaller in amplitude. These observations were validated by the sample-wise permutation testing that revealed significant amplitude differences between the reactive and proactive condition in 170-248 ms and 274-398 ms after stop signal presentation.

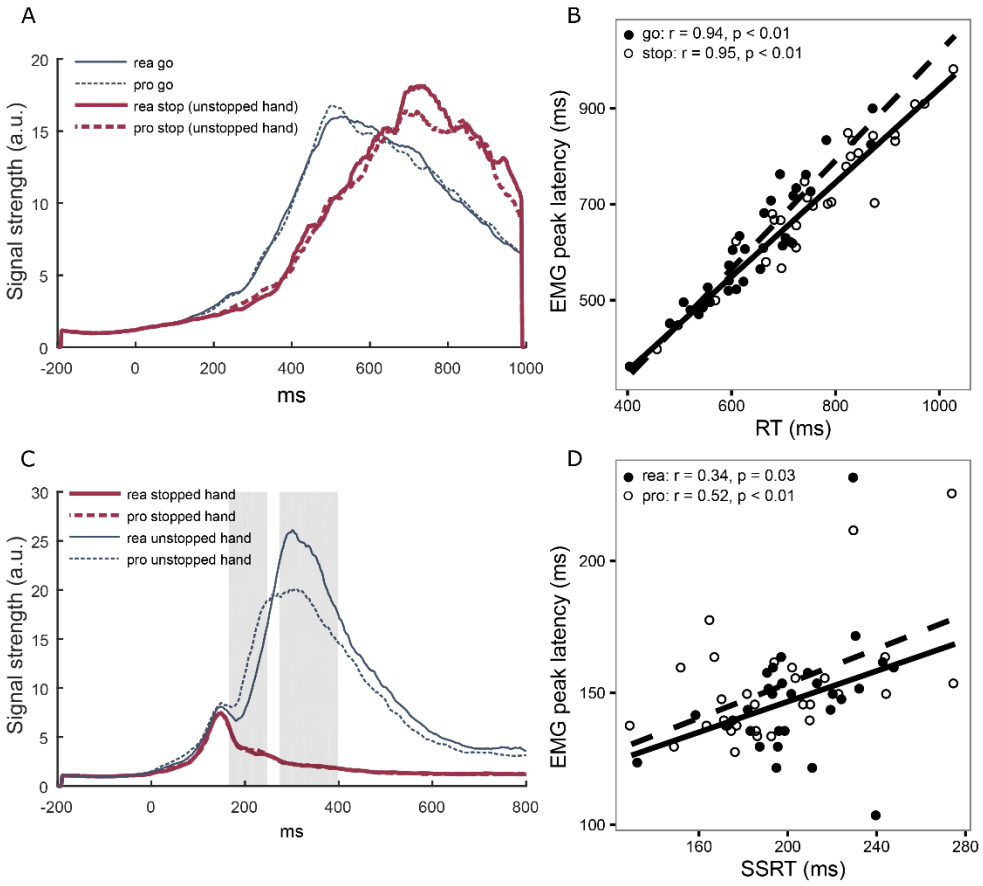

Fig. 2. (a) EMG activity in go and successful stop trials, aligned to go stimuli and depicted as the ratio to the pre-stimulus baseline (b) correlations of the peak EMG latencies (aligned to go stimuli) and corresponding reaction times, including regression line, Pearson correlation coefficients and one-tailed p-values (c) EMG activity in successful stop trials, aligned to stop stimulus presentation and depicted as the ratio to the pre-stimulus baseline; shaded areas depict significant differences between the reactive and proactive condition in the unstopped hand (d) correlations of SSRT and subthreshold EMG activity of stopped hand in successful stop trials, including regression line, Pearson correlation coefficients and one-tailed p-values

The amplitude differences between conditions in the unstopped hand may reflect the continuation of the previous response in the proactive condition, but linear superposition of a newly generated response in the reactive condition. Thus, an additional analysis was carried out with the stop trials aligned to the go stimuli, with the expectation to find similar amplitudes of stop and go trial responses in the proactive condition, but stronger stop than go trial activity in the reactive condition. This analysis confirmed higher stop trial amplitudes in the reactive than in proactive condition ($t(29) = 2.68$, $p = 0.01$, $d = 0.49$), and larger stop than go trial amplitudes both in the reactive ($t(29) = 5.16$, $p < 0.01$, $d = 0.94$) and the proactive ($t(29) = 3.28$, $p < 0.01$, $d = 0.60$) condition.

Electroencephalography

For comparative reasons, original ERPs with topographical maps of the peaks are depicted in Figure 3. We observed the typical ERPs seen in standard stop signal and go/no-go tasks, with marked N2 and P3 in stop conditions, whereas no distinct peak corresponding to the N1 could be observed. However, the topographical maps of stop trials at around 200 ms revealed a diffused negativity across central, parietal and occipital areas, introducing the possibility of a late N1 and its fusion with the subsequent N2. The P3 showed centro-parietal maxima in stop trials.

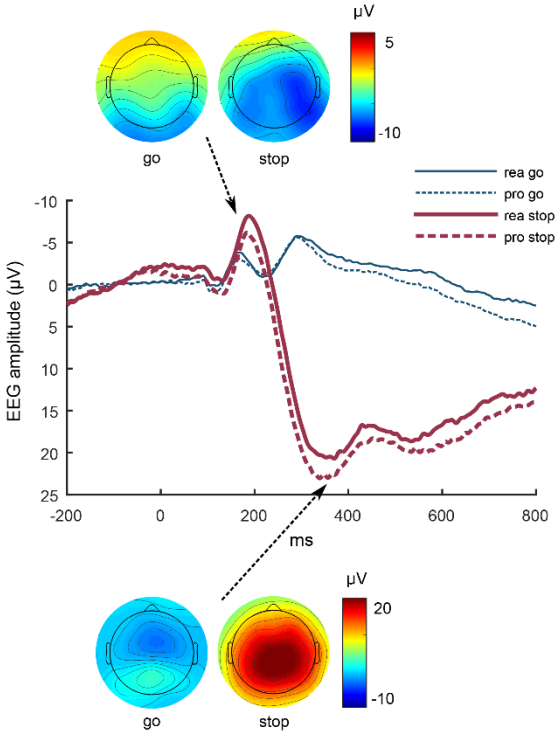

Fig. 3. ERP time-courses in electrode Cz and topographies corresponding to the local peaks at 186-196 ms (top) and 370-380 ms (bottom); negativity is plotted up

Original EEG recordings were decomposed into 15 components, because 15 components accounted for at least 99% of the variance in each participant's data. All 15 components are depicted in the supplementary materials (Figure S1). Based on previous descriptions of the ERPs observed in response inhibition tasks, we were able to identify one component capturing each, the N1 (Figure 4) and N2 (Figure 5), both peaking at around 200 ms after stimulus presentation. In case of the P3, four components showed distinct positivity at around 300 ms with centro-parietal and/or fronto-central

topography (Figure 6). The correlations of the components' amplitudes and onsets with the SSRT and EMG latency are listed in Table 2. In the following, each of those components will be described individually.

N1

Due to its bilateral occipito-parietal activity and distinct negativity starting at 144 ms and peaking at 190 ms in stop trials, component 4 was identified as the N1 (Figure 4A). It explained most variance in the original stop-ERP bilaterally in the posterior electrodes with a maximum of 27% in electrode TP10 (Figure 4C). Its mean amplitudes showed significant main effects for both *trial* ($F(1, 29) = 41.39$, $p < 0.01$, $\eta_p^2 = 0.59$) and *condition* ($F(1,29) = 15.48$, $p < 0.01$, $\eta_p^2 = 0.35$), with stronger amplitudes in stop than in go trials, and in the reactive than in the proactive condition (Figure 4B). No significant correlations emerged regarding the component's amplitude or onset latency and the SSRT or subthreshold EMG latency.

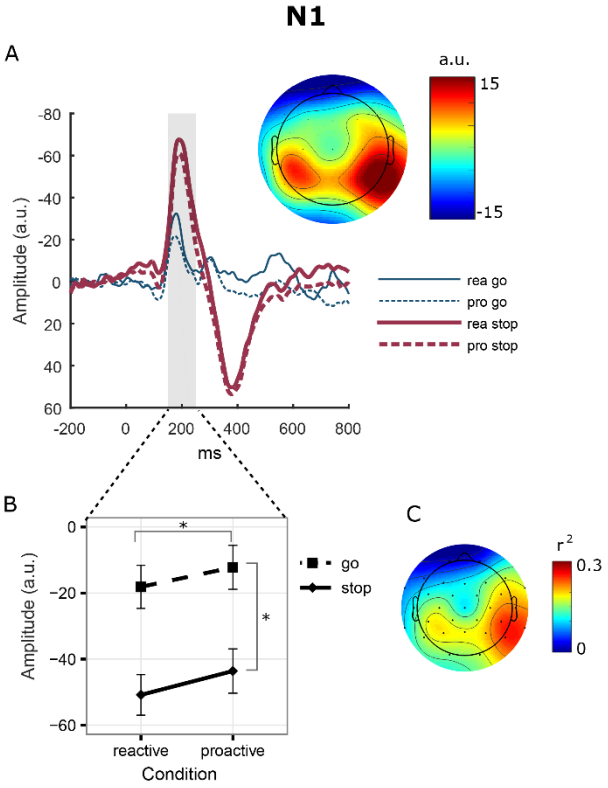

Fig. 4. (a) N1 (component 4) time-courses and its topography; negativity is plotted up; the shaded area marks the time-window of statistical testing (b) Mean amplitudes extracted from the component time-courses; the error bars mark 95% confidence intervals, corrected for repeated measures (c) topographical map representing the variation explained by the component in the original ERP in all electrodes

N2

Component 6 was identified as the N2 due to its fronto-central negativity starting at 133 ms and peaking at 236 ms in stop trials (Figure 5A). Its contribution to the original ERP was rather low, with a maximum of 10% in electrode FC1 (Figure 5C). The main effect of *trial* ($F(1,29) = 24.76$, $p < 0.01$, $\eta_p^2 = 0.46$) was superseded by a significant interaction of *trial* and *condition* ($F(1,29) = 6.77$, $p = 0.01$, $\eta_p^2 = 0.19$; Figure 5B). The post-hocs revealed stronger activations in stop than in go trials (reactive: $t(29) = 5.29$, $p < 0.01$, $d = 0.95$; proactive: $t(29) = 4.45$, $p < 0.01$, $d = 0.81$), but also

that activity in the reactive condition was stronger than proactive only in stop trials (go: t(29) = 0.82, p = 0.42, d = 0.15; stop: t(29) = -3.26, p < 0.01, d = -0.60). Neither the component amplitudes nor the onset latencies correlated with the SSRT of subthreshold EMG latency.

P3

Four separate components emerged with a peak at around 300 ms and centro-parietal and/or fronto-central topographies (Figure 6). They are described in the following, in the order of variance explained in the original ERP.

Component 11 had the strongest activity over centro-parietal electrodes, starting at 217 ms and peaking at 359 ms in stop trials. It explained up to 50% of the variance in electrode CP2, thus largely capturing the early P3 in the original stop-ERP. The main effect of *trial* (F(1,29) = 110.49, p < 0.01, η_p^2 = 0.79) confirmed that stop trial activity was stronger than go trial activity, whereas the main effect of *condition* (F(1,29) = 6.23, p = 0.02, η_p^2 = 0.18) revealed stronger proactive than reactive activity across all trials, although the visualization of this component revealed that this effect seems to be rather driven by the go trial activity. No significant correlations emerged with the SSRT or subthreshold EMG latency.

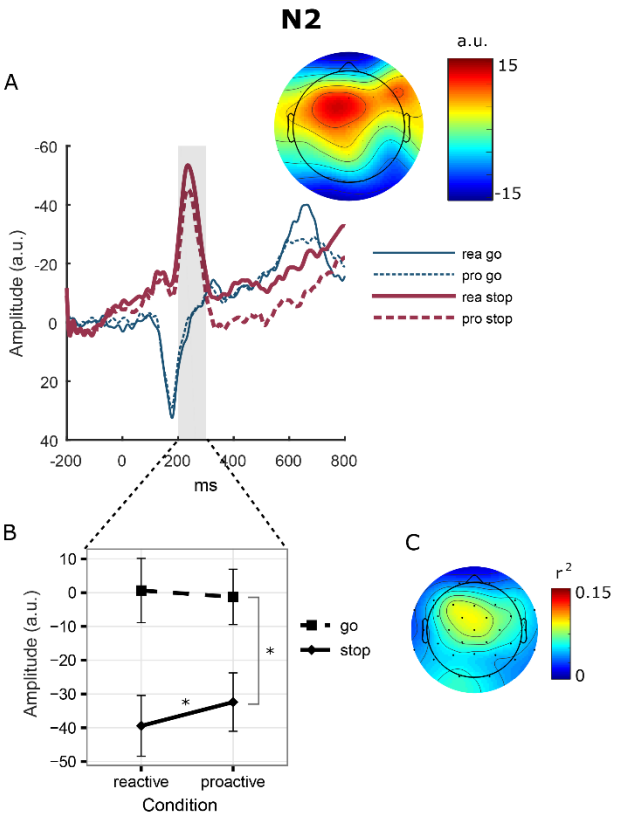

Fig. 5. (a) N2 (component 6) time-courses and its topography; negativity is plotted up; the shaded area marks the time-window of statistical testing; the time-courses and topographies of the component are reversed for visualization purposes so that the time-courses would agree with the standard polarity of the N200 (b) mean amplitudes extracted from the component time-courses; the error bars mark 95% confidence intervals, corrected for repeated measures (c) topographical map representing the variation explained by the component in the original ERP in all electrodes

Component 12 was characterized by a slowly rising positivity in stop trials over fronto-central areas, starting at 189 ms in stop trials with a first peak of activity at around 330 ms followed by a steady

increase in activity. The maximum amount of variance explained in the original stop-ERP was 16% in the electrode FC2. We quantified the activity of the first peak in the time-window of 250-400 ms and found the main effects of *trial* ($F(1, 29 = 59.50$, $p < 0.01$, $\eta_p^2 = 0.67$) and *condition* ($F(1, 29) = 8.19$, $p < 0.01$, $\eta_p^2 = 0.22$), which were further superseded by an interaction of the two ($F(1,29) = 5.38$, $p = 0.03$, $\eta_p^2 = 0.16$). Post-hoc tests revealed that the activity was stronger in stop than in go trials (reactive: $t(29) = 6.97$, $p < 0.01$, $d = 1.27$; proactive: $t(29) = 8.10$, $p < 0.01$, $d = 1.49$), and stronger in the proactive than the reactive condition in stop trials (go: $t(29) = -0.44$, $p = 0.42$, $d = -0.08$; stop: $t(29) = -3.57$, $p < 0.01$, $d = -0.65$). The mean amplitudes correlated negatively with the SSRT in the reactive condition (Table 2), whereas no significant correlations emerged regarding the component onset latency.

Component 10 showed the strongest activity over parietal and occipital areas, starting at 167 ms and peaking at 398 ms in stop trials, but continuing to grow until 686 ms in go trials. A maximum of 14% of the original ERP-variance was explained in electrode Pz. No main effects of the trial type or condition occurred, but there was a significant interaction of the two ($F(1,29) = 4.21$, $p = 0.05$, $\eta_p^2 = 0.13$). However, no comparison survived the correction for multiple comparisons in post-hoc testing, indicating similar levels of activation across go and stop trials, and in reactive and proactive conditions.

Component 8 exhibited a very concise fronto-central topography starting at 155 ms and peaking at 292 ms in stop trials. It explained maximally 12% of the original stop-ERP variance in electrode Fz. There was a significant main effect of the factor *trial* ($F(1,29) = 39.67$, $p < 0.01$, $\eta_p^2 = 0.58$), where activity in stop trials was stronger than in go trials. The main effect of *condition* ($F(1, 29) = 8.06$, $p < 0.01$, $\eta_p^2 = 0.22$) confirmed that proactive activity was larger than reactive activity across all trials. This component's stop trial amplitude correlated negatively with the SSRT both in the reactive and proactive condition, and with subthreshold EMG latency in the proactive condition (Table 2). Its onset latency also correlated with the SSRT in the proactive condition; though the direction of this correlation was negative, relating faster component onset to delayed inhibition.

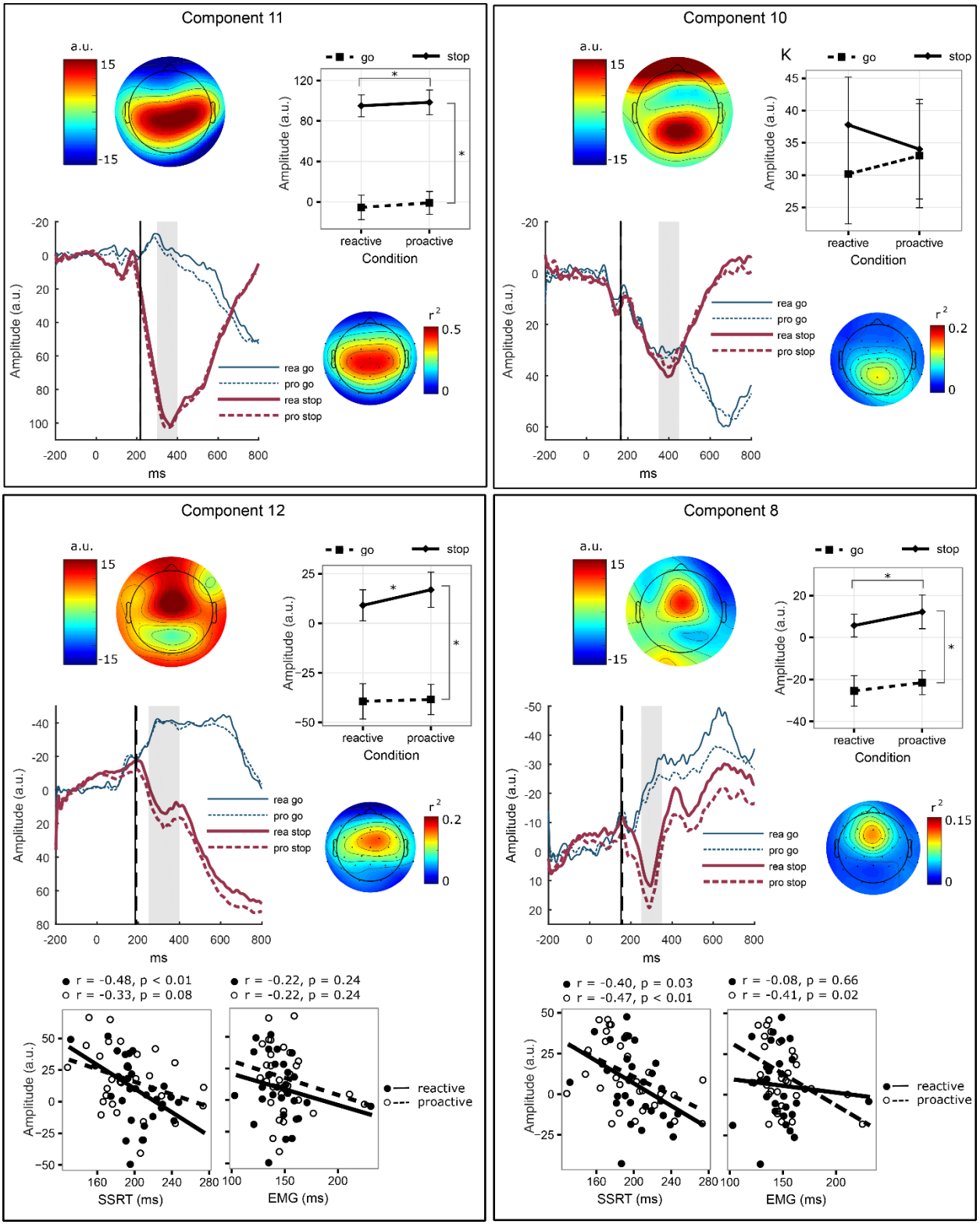
Component 11
a.u.
15
-15
go
stop
Amplitude (a.u.)
reactive
proactive
Condition
rea go
pro go
rea stop
pro stop
ms
r²
0.5
0
Component 10
K
0.2
Component 12
r = -0.48, p < 0.01
r = -0.33, p = 0.08
r = -0.22, p = 0.24
r = -0.22, p = 0.24
SSRT (ms)
EMG (ms)
Component 8
r = -0.40, p = 0.03
r = -0.47, p < 0.01
r = -0.08, p = 0.66
r = -0.41, p = 0.02
0.15

Fig. 6. P3-like components; the upper left panels in each component depict the component topographies and the lower (components 11 and 10) or middle (components 12 and 8) left panels depict the component time-courses, with negativity plotted up; the shaded areas mark the time-windows of statistical testing and the vertical lines mark the onsets of the components; upper right panels depict the mean amplitudes extracted from the component time-courses; the error bars mark 95% confidence intervals, corrected for repeated measures; the lower (components 11 and 10) or middle (components 12 and 8) right panels depict the topographical maps representing the variation explained by the component in the original ERP in all electrodes; the lower panels by component 12 and 8 show the Pearson correlations and regression lines of the component activities with the SSRTs and subthreshold EMG interruption latencies (N = 30)

	SSRT		**EMG**	
	Reactive	Proactive	Reactive	Proactive
Amplitude				
Comp 4 (N1)	.04	.34	.08	-.01
Comp 6 (N2)	.12	.19	.01	-.10
Comp 11 (P3)	-.31	.00	.25	.02
Comp 12 (P3)	**-.48****	-.33	-.22	-.22
Comp 10 (P3)	.18	.21	.23	.02
Comp 8 (P3)	**-.40***	**-.47****	-.08	**-.41***
Onset				
Comp 4 (N1)	.20	-.11	-.13	.06
Comp 6 (N2)	.26	-.29	.11	-.18
Comp 11 (P3)	-.25	-.05	-.11	.19
Comp 12 (P3)	-.24	-.27	-.36	-.14
Comp 10 (P3)	.13	.20	.13	.02
Comp 8 (P3)	-.18	**-.42***	-.16	-.35

Table 2. Pearson correlation coefficients for EEG components with the SSRTs and subthreshold EMG interruption latencies (n = 30). * $p < 0.05$, ** $p < 0.01$

Discussion

We compared the neural modulations of the inhibitory system by reactive and proactive control modes, focusing on the temporal progression of selective inhibition. Complementary to the SSRT estimation, we utilized EMG recordings as a measure of individual inhibition latency and found that inhibition is exerted at the effector level at around 150 ms after stop stimulus presentation, in contrast to SSRT which was estimated to be around 200 ms. Contrary to our hypothesis, no differences in inhibition latencies were found between the reactive and proactive control, whereas both behavioral and EMG results did show less interference on ongoing motor activity in the proactive condition. As for the EEG, group-SOBI revealed that multiple temporally overlapping neural components were modulated by the control modes. As such, P3-like activity was distributed over four components, two of which were associated with behavioral or EMG markers of inhibition, and three of which showed augmented activity in the proactive, as compared to the reactive condition. In contrast, N1 and N2 were larger in the reactive condition. Altogether, this pattern suggests a preferential association of the N1 and N2 with the reactive, and the P3 with the proactive mode of cognitive control.

Latency of successful stopping

The stop signal task has enjoyed an abiding popularity for the study of motor inhibition, mainly due to the possibility of calculating the SSRT that gives an estimate of individual stopping capabilities, shown to differ between various disease states as well as motivational contexts (Locke and Braver 2008; Leotti and Wager 2010; Lipszyc and Schachar 2010; Greenhouse and Wessel 2013; Smittenaar et al. 2013). Given the limitations of the horse race model in complex settings, we exploited the EMG measurements to derive a complementary measure of inhibition latency. Subthreshold EMG activity was detected in 47% of the stop trials without overt response, and this activity was interrupted at around 150 ms after the top signal. Our findings are fully in line with previous TMS studies that have estimated the onset of cortical inhibition to fall between 130 and 175 ms (Coxon et al. 2006; van den Wildenberg et al. 2010; Macdonald et al. 2014). At the same time, a near-perfect match was observed between overt behavioral responses as measured by the reaction times and the EMG measures following a temporal smoothing procedure (Figure 2B), adding confidence to the parametrization of the subthreshold EMG activity.

Together, these findings suggest that inhibition occurs considerably earlier than estimated by the SSRT. Recent experimental and computational advances have highlighted the importance of perceptual processes for successful stopping, and further that the SSRT itself may mostly reflect sensory stimulus processing (Salinas and Stanford 2013; Verbruggen et al. 2014b; Logan et al. 2015). In contrast, assuming that response inhibition is a multistage process including both sensory and motor counterparts, some variability in the EMG latency is necessarily due to the motor processes. The early suppression of the motor activity is thus particularly noteworthy, as it appears to coincide with early action selection processes: alternative accounts of motor control have suggested that instead of active response inhibition, motor cancellation is achieved either by interrupting the maintenance of the current motor plan, or by asymmetric mutual inhibition of competing response tendencies (Band and van Boxtel 1999; Munakata et al. 2011; Verbruggen et al. 2014a). As such, the investigation of the neural underpinnings of inhibition must necessarily be shifted to earlier time points, focusing on how the sensory information is translated into motor plans, and thus also into the modulation, override, or cancellation of a prepared plan.

Selective stopping in the reactive and proactive control modes

Contrary to our expectations, the SSRTs and EMG latencies were similar across both control modes, challenging the hypothetical dichotomy between the fast global and slow selective inhibitory system operating within the reactive and proactive control mode, respectively. At the same time, we did replicate the rather robust results of smaller response costs in the proactive condition as indicated by a decrease in the SI effect (Aron and Verbruggen 2008; Ko and Miller 2011, 2013; Smittenaar et al. 2013; Lavallee et al. 2014); a result that has been previously interpreted as an evidence for the recruitment of the slow selective inhibitory system by proactive control. Complementary evidence from EMG enables an elaboration of this interpretation. Macdonald et al. (2012, 2014) have demonstrated patterns of EMG as well as TMS that correspond to the so-called restart model of selective stopping, where the activation of the unstopped hand was suppressed shortly after the stop stimulus, followed by a new rise in the activation corresponding to the given response. We observed exactly the same pattern of the unstopped hand's EMG in the reactive condition, implying global stopping of all ongoing motor actions and the re-initiation of a new response. In the proactive condition though, there was less interference on the unstopped hand EMG activity, as well as reduced amplitudes of the unstopped hand EMG response as compared to the reactive condition (Figure 2C). The amplitude differences between the reactive and proactive condition persisted when the EMG

activity was time-locked to go trials, whereas unstopped hand EMG responses had still larger amplitudes than normal go responses, potentially reflecting a linear superposition of the cancelled and a newly generated response (Figure 2C). Thus, our data fully support the restart model of selective stopping in the reactive condition. In the proactive condition, ongoing motor activity also seems to be susceptible to inhibitory interference, but to a lesser degree, putatively causing a temporal halt as opposed to a full suppression of the prepared response.

Modulations of event-related potentials

The ERPs revealed the N2/P3 complex typically seen in response inhibition tasks (Figure 3). No clear N1 was observed in the original ERPs - a pattern not uncommon in visual stop signal tasks (Kenemans 2015). The topographical maps at around 200 ms, however, showed a distributed negativity across central and posterior scalp areas, suggesting a contribution from several simultaneously active neural generators. Indeed, group-SOBI could efficiently isolate temporally overlapping neural events, resulting in a distinction between a bilateral occipital and a fronto-central component in the time-frame at around 150-250 ms, which we identified as N1 and N2, respectively (Figures 4 and 5). Similarly, the decomposition via SOBI resulted in four distinct components that, due to their fronto-central and/or centro-parietal topography and marked positivity at around 300 ms, were considered as potential contributors to the stop-related P3 (Figure 6).

N1

A stronger N1 was observed in the reactive as opposed to the proactive condition, although the opposite was excepted due to strategic orientation of attention to stimulus-related features in the proactive condition (Greenhouse and Wessel 2013; Schevernels et al. 2015; Langford et al. 2016a, b). However, given that the N1 also tends to be larger in case of visual discrimination, as compared to detection (Vogel and Luck 2000), our results are not completely at odds. In the current task, the preparatory cues were spatially specific, thus the decision which hand may need to be stopped was shifted to the cue onset in the proactive condition, but to stop stimulus onset in the reactive condition, introducing an additional target discrimination stage in the reactive condition. On the other hand, we also observed a stronger N1 in the reactive condition in go trials where the response was always bimanual, suggesting a more complex relationship between the N1 and the control modes which may be dependent on the specific task context.

N2

Agreeing with our hypothesis, the N2 was stronger in the reactive than in the proactive condition. The N2 is thought to reflect conflict detection between multiple competing response representations, i.e. between go and stop processes in the stop trials (Folstein and Van Petten 2008; Ullsperger et al. 2014). The reduced N2 amplitudes in the proactive condition thus likely reflect smaller conflict due to preparative cues.

P3

Four components showed P3-like activity which is in agreement with the notion that the P3 is generated by multiple neuronal sources (Johnson 1993; Nieuwenhuis et al. 2005; Polich 2007). Much of the original P3 ERP was explained by components 11 and 12, likely corresponding to the already established distinction of the early P3a and late P3b, respectively (Polich 2007). The other two P3-like components, 8 and 10, explained smaller portions of the original ERP variance and may thus not be identifiable in the standard ERP analyses.

Three out of four P3-like components, component 11, 12 and 8, showed augmented activity in the proactive condition, whereas it was specific to stop trials only in component 12. Of these three, the amplitudes of components 12 and 8, but not their onsets, correlated with the SSRT (and with proactive EMG in the case of component 8), relating stronger amplitude to faster inhibition. Given that both of the components' onsets were identified well before the SSRT (151 and 184 ms for components 8 and 12, respectively) as well as the recent reports of strong correlations between the P3 onsets and the SSRT (Wessel and Aron 2014; Wessel et al. 2016), the lack of the association between the component onsets and SSRT in the present study may seem disconcerting at first. Yet, this discrepancy may be driven by several methodological differences between the studies. Firstly, we defined the component onsets as the latency of 10% of the area under the curve, thus being independent of go trial activity, whereas Wessel and Aron defined the onset as the first significant time-point between go and stop ERPs. Secondly, we applied group-SOBI for data decomposition, as opposed to single-subject ICA solutions with subsequent matching of the components between participants. Group-level BSS techniques have the advantage of an inherent component matching across subjects such that each participant has an individual time-course across all the derived components, thereby reducing mere subjective decisions in component matching if some subjects should show several (or none) P3-like components. Thirdly, it may well be that the mechanisms driving the P3 behave differently in a selective stop signal task. Most importantly, though, our EMG

results imply that inhibition occurs well before the SSRT, casting doubt on the postulation of the P3 as an online index of response inhibition.

Yet, the P3 does evidently co-vary with inhibition processes as shown by the correlations of P3 amplitudes with the SSRT and EMG, delayed P3 latency in unsuccessful stopping (Dimoska et al. 2006), and decreased P3 amplitudes accompanied by prolonged SSRTs in patients with ADHD (Bekker et al. 2005b). The partitioning of the P3 as shown here suggests that only a fraction of the neural processes that contribute to the P3 may be associated with response inhibition. Alternatively, there is also the possibility of mutual dependencies between the processes driving the P3 and earlier inhibitory activity. Compelling evidence comes from a recent effective connectivity study where an independent component capturing much of the later-occurring P3 variance exerted early causal influence on the desynchronization of occipital alpha (Huster et al. 2014). Together with the augmented activity in the proactive condition, it implies that the mechanisms driving the P3 rather reflect fluctuations in attentional and feedback-related networks, which nevertheless interact with earlier inhibitory processes that are sensitive to top-down attentional modulation and/or may influence the (inhibitory) processing of stimuli in the following trials.

Conclusions

Our results suggest that the suppression of selective responses can be fast, occurring as early as 150 ms. The inhibition latency was similar in the reactive and proactive control mode, challenging the temporal argument for the mapping of selective and global inhibition to the reactive and proactive control modes, respectively. The behavioral and EMG results both agree with the restart model of selective stopping in the reactive condition, stating that all responses are suppressed globally and the correct response is newly generated thereafter. In contrast, proactive control seemed to result in the halt and continuation of the ongoing actions, rather than total suppression and generation of a new response. These observations were paralleled by amplitude modulations of ERP components where the reactive mode was associated with augmented N1 and N2, and the proactive mode with stronger P3 activity. Whereas two out of four neural generators driving the P3 did correlate with inhibition latency, their late appearance relative to the subthreshold EMG and SSRT suggest that they are rather indicative of post-inhibition attention-modulated processes. Thus, to fully characterize the cascade of events resulting in response inhibition, a shift towards investigating the neural activity at the earlier time-frames seems essential.

Ethical approval: All procedures performed in studies involving human participants were in accordance with the ethical standards of the institutional and/or national research committee and with the 1964 Helsinki declaration and its later amendments or comparable ethical standards.

References

Albares M, Lio G, Criaud M, et al (2014) The dorsal medial frontal cortex mediates automatic motor inhibition in uncertain contexts: evidence from combined fMRI and EEG studies. Hum Brain Mapp 35:5517–5531. doi: 10.1002/hbm.22567

Aron AR (2011) From reactive to proactive and selective control: developing a richer model for stopping inappropriate responses. Biol Psychiatry 69:e55-68. doi: 10.1016/j.biopsych.2010.07.024

Aron AR, Verbruggen F (2008) Stop the presses: dissociating a selective from a global mechanism for stopping. Psychol Sci 19:1146–1153. doi: 10.1111/j.1467-9280.2008.02216.x

Band GP, van Boxtel GJ (1999) Inhibitory motor control in stop paradigms: review and reinterpretation of neural mechanisms. Acta Psychol (Amst) 101:179–211.

Band GPH, van der Molen MW, Logan GD (2003) Horse-race model simulations of the stop-signal procedure. Acta Psychol (Amst) 112:105–142.

Bekker EM, Kenemans JL, Hoeksma MR, et al (2005a) The pure electrophysiology of stopping. Int J Psychophysiol Off J Int Organ Psychophysiol 55:191–198. doi: 10.1016/j.ijpsycho.2004.07.005

Bekker EM, Overtoom CCE, Kooij JJS, et al (2005b) Disentangling deficits in adults with attention-deficit/hyperactivity disorder. Arch Gen Psychiatry 62:1129–1136. doi: 10.1001/archpsyc.62.10.1129

Belouchrani A, Abed-Meraim K, Cardoso J-F, Moulines E (1997) A Blind Source Separation Technique Using Second-order Statistics. Trans Sig Proc 45:434–444. doi: 10.1109/78.554307

Benjamini Y, Hochberg Y (1995) Controlling the False Discovery Rate: A Practical and Powerful Approach to Multiple Testing. J R Stat Soc Ser B Methodol 57:289–300.

Bissett PG, Logan GD (2014) Selective stopping? Maybe not. J Exp Psychol Gen 143:455–472. doi: 10.1037/a0032122

Boehler CN, Appelbaum LG, Krebs RM, et al (2012) The influence of different Stop-signal response time estimation procedures on behavior-behavior and brain-behavior correlations. Behav Brain Res 229:123–130. doi: 10.1016/j.bbr.2012.01.003

Boehler CN, Münte TF, Krebs RM, et al (2009) Sensory MEG responses predict successful and failed inhibition in a stop-signal task. Cereb Cortex N Y N 1991 19:134–145. doi: 10.1093/cercor/bhn063

Braver TS (2012) The variable nature of cognitive control: a dual mechanisms framework. Trends Cogn Sci 16:106–113. doi: 10.1016/j.tics.2011.12.010

Burle B, Possamaï C-A, Vidal F, et al (2002) Executive control in the Simon effect: an electromyographic and distributional analysis. Psychol Res 66:324–336. doi: 10.1007/s00426-002-0105-6

Cai W, Oldenkamp CL, Aron AR (2011) A proactive mechanism for selective suppression of response tendencies. J Neurosci Off J Soc Neurosci 31:5965–5969. doi: 10.1523/JNEUROSCI.6292-10.2011

Claffey MP, Sheldon S, Stinear CM, et al (2010) Having a goal to stop action is associated with advance control of specific motor representations. Neuropsychologia 48:541–548. doi: 10.1016/j.neuropsychologia.2009.10.015

Cohen MX, van Gaal S (2014) Subthreshold muscle twitches dissociate oscillatory neural signatures of conflicts from errors. NeuroImage 86:503–513. doi: 10.1016/j.neuroimage.2013.10.033

Congdon E, Mumford JA, Cohen JR, et al (2012) Measurement and reliability of response inhibition. Front Psychol 3:37. doi: 10.3389/fpsyg.2012.00037

Coxon JP, Stinear CM, Byblow WD (2007) Selective inhibition of movement. J Neurophysiol 97:2480–2489. doi: 10.1152/jn.01284.2006

Coxon JP, Stinear CM, Byblow WD (2006) Intracortical inhibition during volitional inhibition of prepared action. J Neurophysiol 95:3371–3383. doi: 10.1152/jn.01334.2005

De Jong R, Coles MG, Logan GD, Gratton G (1990) In search of the point of no return: the control of response processes. J Exp Psychol Hum Percept Perform 16:164–182.

Delorme A, Makeig S (2004) EEGLAB: an open source toolbox for analysis of single-trial EEG dynamics including independent component analysis. J Neurosci Methods 134:9–21. doi: 10.1016/j.jneumeth.2003.10.009

Dimoska A, Johnstone SJ, Barry RJ (2006) The auditory-evoked N2 and P3 components in the stop-signal task: indices of inhibition, response-conflict or error-detection? Brain Cogn 62:98–112. doi: 10.1016/j.bandc.2006.03.011

Dimoska A, Johnstone SJ, Barry RJ, Clarke AR (2003) Inhibitory motor control in children with attention-deficit/hyperactivity disorder: event-related potentials in the stop-signal paradigm. Biol Psychiatry 54:1345–1354.

Donkers FCL, van Boxtel GJM (2004) The N2 in go/no-go tasks reflects conflict monitoring not response inhibition. Brain Cogn 56:165–176. doi: 10.1016/j.bandc.2004.04.005

Eichele T, Rachakonda S, Brakedal B, et al (2011) EEGIFT: Group Independent Component Analysis for Event-Related EEG Data. Comput Intell Neurosci. doi: 10.1155/2011/129365

Enriquez-Geppert S, Konrad C, Pantev C, Huster RJ (2010) Conflict and inhibition differentially affect the N200/P300 complex in a combined go/nogo and stop-signal task. NeuroImage 51:877–887. doi: 10.1016/j.neuroimage.2010.02.043

Filipović SR, Jahanshahi M, Rothwell JC (2000) Cortical potentials related to the nogo decision. Exp Brain Res 132:411–415.

Folstein JR, Van Petten C (2008) Influence of cognitive control and mismatch on the N2 component of the ERP: a review. Psychophysiology 45:152–170. doi: 10.1111/j.1469-8986.2007.00602.x

Greenhouse I, Wessel JR (2013) EEG signatures associated with stopping are sensitive to preparation. Psychophysiology 50:900–908. doi: 10.1111/psyp.12070

Gulberti A, Arndt PA, Colonius H (2014) Stopping eyes and hands: evidence for non-independence of stop and go processes and for a separation of central and peripheral inhibition. Front Hum Neurosci 8:61. doi: 10.3389/fnhum.2014.00061

Hasbroucq T, Possamaï CA, Bonnet M, Vidal F (1999) Effect of the irrelevant location of the response signal on choice reaction time: an electromyographic study in humans. Psychophysiology 36:522–526.

Huster RJ, Enriquez-Geppert S, Lavallee CF, et al (2013) Electroencephalography of response inhibition tasks: functional networks and cognitive contributions. Int J Psychophysiol Off J Int Organ Psychophysiol 87:217–233. doi: 10.1016/j.ijpsycho.2012.08.001

Huster RJ, Plis SM, Calhoun VD (2015) Group-level component analyses of EEG: validation and evaluation. Front Neurosci 9:254. doi: 10.3389/fnins.2015.00254

Huster RJ, Plis SM, Lavallee CF, et al (2014) Functional and effective connectivity of stopping. NeuroImage 94:120–128. doi: 10.1016/j.neuroimage.2014.02.034

Huster RJ, Schneider S, Lavallee CF, et al (2016) Filling the void—enriching the feature space of successful stopping. Hum Brain Mapp n/a-n/a. doi: 10.1002/hbm.23457

Hyvärinen A, Oja E (2000) Independent component analysis: algorithms and applications. Neural Netw Off J Int Neural Netw Soc 13:411–430.

Jahfari S, Waldorp L, van den Wildenberg WPM, et al (2011) Effective connectivity reveals important roles for both the hyperdirect (fronto-subthalamic) and the indirect (fronto-striatal-pallidal) fronto-basal ganglia pathways during response inhibition. J Neurosci Off J Soc Neurosci 31:6891–6899. doi: 10.1523/JNEUROSCI.5253-10.2011

Johnson R (1993) On the neural generators of the P300 component of the event-related potential. Psychophysiology 30:90–97.

Kenemans JL (2015) Specific proactive and generic reactive inhibition. Neurosci Biobehav Rev 56:115–126. doi: 10.1016/j.neubiorev.2015.06.011

Ko Y-T, Miller J (2011) Nonselective motor-level changes associated with selective response inhibition: evidence from response force measurements. Psychon Bull Rev 18:813–819. doi: 10.3758/s13423-011-0090-0

Ko Y-T, Miller J (2013) Signal-related contributions to stopping-interference effects in selective response inhibition. Exp Brain Res 228:205–212. doi: 10.1007/s00221-013-3552-y

Langford ZD, Krebs RM, Talsma D, et al (2016a) Strategic down-regulation of attentional resources as a mechanism of proactive response inhibition. Eur J Neurosci. doi: 10.1111/ejn.13303

Langford ZD, Schevernels H, Boehler CN (2016b) Motivational context for response inhibition influences proactive involvement of attention. Sci Rep 6:35122. doi: 10.1038/srep35122

Lavallee CF, Meemken MT, Herrmann CS, Huster RJ (2014) When holding your horses meets the deer in the headlights: time-frequency characteristics of global and selective stopping under conditions of proactive and reactive control. Front Hum Neurosci 8:994. doi: 10.3389/fnhum.2014.00994

Leotti LA, Wager TD (2010) Motivational influences on response inhibition measures. J Exp Psychol Hum Percept Perform 36:430–447. doi: 10.1037/a0016802

Lio G, Boulinguez P (2013) Greater robustness of second order statistics than higher order statistics algorithms to distortions of the mixing matrix in blind source separation of human EEG: implications for single-subject and group analyses. NeuroImage 67:137–152. doi: 10.1016/j.neuroimage.2012.11.015

Lipszyc J, Schachar R (2010) Inhibitory control and psychopathology: a meta-analysis of studies using the stop signal task. J Int Neuropsychol Soc JINS 16:1064–1076. doi: 10.1017/S1355617710000895

Locke HS, Braver TS (2008) Motivational influences on cognitive control: behavior, brain activation, and individual differences. Cogn Affect Behav Neurosci 8:99–112.

Logan GD, Cowan WB (1984) On the ability to inhibit thought and action: A theory of an act of control. Psychol Rev 91:295–327. doi: 10.1037/0033-295X.91.3.295

Logan GD, Yamaguchi M, Schall JD, Palmeri TJ (2015) Inhibitory control in mind and brain 2.0: blocked-input models of saccadic countermanding. Psychol Rev 122:115–147. doi: 10.1037/a0038893

Macdonald HJ, Coxon JP, Stinear CM, Byblow WD (2014) The Fall and Rise of Corticomotor Excitability with Cancellation and Reinitiation of Prepared Action. J Neurophysiol. doi: 10.1152/jn.00366.2014

Macdonald HJ, Stinear CM, Byblow WD (2012) Uncoupling response inhibition. J Neurophysiol 108:1492–1500. doi: 10.1152/jn.01184.2011

Majid DSA, Cai W, Corey-Bloom J, Aron AR (2013) Proactive selective response suppression is implemented via the basal ganglia. J Neurosci Off J Soc Neurosci 33:13259–13269. doi: 10.1523/JNEUROSCI.5651-12.2013

Majid DSA, Cai W, George JS, et al (2012) Transcranial magnetic stimulation reveals dissociable mechanisms for global versus selective corticomotor suppression underlying the stopping of action. Cereb Cortex N Y N 1991 22:363–371. doi: 10.1093/cercor/bhr112

Munakata Y, Herd SA, Chatham CH, et al (2011) A unified framework for inhibitory control. Trends Cogn Sci 15:453–459. doi: 10.1016/j.tics.2011.07.011

Nieuwenhuis S, Aston-Jones G, Cohen JD (2005) Decision making, the P3, and the locus coeruleus-norepinephrine system. Psychol Bull 131:510–532. doi: 10.1037/0033-2909.131.4.510

Nieuwenhuis S, Yeung N, van den Wildenberg W, Ridderinkhof KR (2003) Electrophysiological correlates of anterior cingulate function in a go/no-go task: effects of response conflict and trial type frequency. Cogn Affect Behav Neurosci 3:17–26.

Nunez PL, Srinivasan R, Westdorp AF, et al (1997) EEG coherency. I: Statistics, reference electrode, volume conduction, Laplacians, cortical imaging, and interpretation at multiple scales. Electroencephalogr Clin Neurophysiol 103:499–515.

Oldfield RC (1971) The assessment and analysis of handedness: the Edinburgh inventory. Neuropsychologia 9:97–113.

Onton J, Westerfield M, Townsend J, Makeig S (2006) Imaging human EEG dynamics using independent component analysis. Neurosci Biobehav Rev 30:808–822. doi: 10.1016/j.neubiorev.2006.06.007

Polich J (2007) Updating P300: an integrative theory of P3a and P3b. Clin Neurophysiol Off J Int Fed Clin Neurophysiol 118:2128–2148. doi: 10.1016/j.clinph.2007.04.019

Salinas E, Stanford TR (2013) The Countermanding Task Revisited: Fast Stimulus Detection Is a Key Determinant of Psychophysical Performance. J Neurosci 33:5668–5685. doi: 10.1523/JNEUROSCI.3977-12.2013

Schall JD, Godlove DC (2012) Current advances and pressing problems in studies of stopping. Curr Opin Neurobiol 22:1012–1021. doi: 10.1016/j.conb.2012.06.002

Schevernels H, Bombeke K, Van der Borght L, et al (2015) Electrophysiological evidence for the involvement of proactive and reactive control in a rewarded stop-signal task. NeuroImage 121:115–125. doi: 10.1016/j.neuroimage.2015.07.023

Smittenaar P, Guitart-Masip M, Lutti A, Dolan RJ (2013) Preparing for selective inhibition within frontostriatal loops. J Neurosci Off J Soc Neurosci 33:18087–18097. doi: 10.1523/JNEUROSCI.2167-13.2013

Smittenaar P, Rutledge RB, Zeidman P, et al (2015) Proactive and Reactive Response Inhibition across the Lifespan. PloS One 10:e0140383. doi: 10.1371/journal.pone.0140383

Ullsperger M, Danielmeier C, Jocham G (2014) Neurophysiology of Performance Monitoring and Adaptive Behavior. Physiol Rev 94:35–79. doi: 10.1152/physrev.00041.2012

van den Wildenberg WPM, Burle B, Vidal F, et al (2010) Mechanisms and dynamics of cortical motor inhibition in the stop-signal paradigm: a TMS study. J Cogn Neurosci 22:225–239. doi: 10.1162/jocn.2009.21248

Verbruggen F, Chambers CD, Logan GD (2013) Fictitious inhibitory differences: how skewness and slowing distort the estimation of stopping latencies. Psychol Sci 24:352–362. doi: 10.1177/0956797612457390

Verbruggen F, Logan GD (2015) Evidence for capacity sharing when stopping. Cognition 142:81–95. doi: 10.1016/j.cognition.2015.05.014

Verbruggen F, McLaren IPL, Chambers CD (2014a) Banishing the Control Homunculi in Studies of Action Control and Behavior Change. Perspect Psychol Sci J Assoc Psychol Sci 9:497–524. doi: 10.1177/1745691614526414

Verbruggen F, Stevens T, Chambers CD (2014b) Proactive and reactive stopping when distracted: An attentional account. J Exp Psychol Hum Percept Perform 40:1295–1300. doi: 10.1037/a0036542

Vogel EK, Luck SJ (2000) The visual N1 component as an index of a discrimination process. Psychophysiology 37:190–203.

Wessel JR, Aron AR (2014) It's not too late: The onset of the frontocentral P3 indexes successful response inhibition in the stop-signal paradigm. Psychophysiology. doi: 10.1111/psyp.12374

Wessel JR, Jenkinson N, Brittain J-S, et al (2016) Surprise disrupts cognition via a fronto-basal ganglia suppressive mechanism. Nat Commun 7:11195. doi: 10.1038/ncomms11195